

Wave packet dynamics

(Dated: December 16, 2013)

PACS numbers:

Contents

I. About this note	1
II. Some preliminary related observations/considerations	1
A. Scaling of the Fibonacci polariton spectrum	1
B. Time scales of scaling vs lifetime	2
III. Literature review	2
A. List of some literature in the chronological order:	2
B. System length (# of observed LPO periods vs Fibonacci generation)	4
C. Numerical experiment time scale vs energy scales of the spectrum	4
D. Choice of the initial site position	4
IV. Theoretical background	5
A. Usually considered quantities	5
B. Auto-correlation function (mean return probability) $C(t)$	5
C. The RMS displacement and the participation ratio	7
V. Some preliminary numerical results	7
VI. Systematic numerical simulations	8
A. Method of numerical simulation	8
B. Numerical results	9
VII. Some ideas	10
A. Resonant tunneling propagation and non-linear effects	10
B. Analogue of the spontaneous emission	12
References	12

I. ABOUT THIS NOTE

This note is dedicated to the possibility of the observation of the log-periodic features in the dynamics of the wave packet expansion in a quasi-periodic 1D polariton wire. The considered system length matches that used in the experimental system. i.e. S_{12} counting 144 letters (plus the wire padding). (Wire padding, is not removed, since it is not expected to affect strongly the wave packet dynamics, - because the related edge states do not participate the spectral expansion of the initial packet).

II. SOME PRELIMINARY RELATED OBSERVATIONS/CONSIDERATIONS

A. Scaling of the Fibonacci polariton spectrum

The experimental system is considered, i.e. S_{12} counting 144 letters. For this system, more or less "pure" scaling is obtained in the lowest sub-band with three scaling cycles (scaling about the lowest state in the sub-band). The corresponding energy scaling factor is about 20. Then, much less pure but analogous scaling can be found in the 2nd and the 3rd sub-bands, Fig. 1, with the "mean" scaling factors of about 10 and 7. These scaling are less "pure" since the sub-bands are much wider. The latter affects the uniformity of the scaling within the sub-bands, but the difference in the scaling factors between the sub-bands is seemingly related to the multi-fractality.

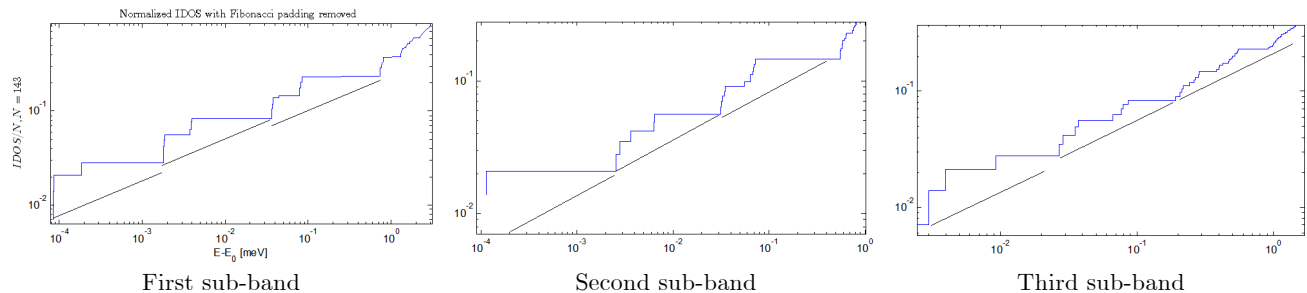


FIG. 1: Scaling of the 1st, 2nd and 3rd sub-bands relative to the lower sub-band edge. Equal-length line segments are shown to demonstrate scaling non-uniformity.

B. Time scales of scaling vs lifetime

The DOS scaling is valid in some range of energy scales. In the idealized experimental system analogue they range (see above) from about 10^{-4} meV to ~ 1 meV. This values are directly related to the corresponding time scales of the log-periodic behavior (at least for the return probability). In order that this behavior could be observed, we need that the polariton life time would be of the order or longer than those time scales. We know that the inverse life time is of the order of 0.1 meV, which, at best, leaves us only one period of the log-periodic oscillations (LPO) (unless, by some improbable magic/coincidence the whole three-band structure would yield one more period at yet smaller times).

Thus, if the LPO are possible in principal, then either the life-time of the polaritons should be increased, or energy scale of the self-similar structures in the spectrum should be increased (e.g. by lowering the effective mass, or decreasing the letter length). Another possibility is to somehow engineer the DOS to have scaling symmetry extended over the three main bands.

III. LITERATURE REVIEW

A. List of some literature in the chronological order:

1. Ref. [1]: S. Abe and H. Hiramoto, "Fractal dynamics of electron wave packets in one-dimensional quasi-periodic systems", Phys. Rev. A **36**, 5349 (1987).
 - Seemingly the first (or one of the first) work on the dynamical implications of the fractal spectrum.
 - The off-diagonal 1D tight-binding Fibonacci model (2000 sites) is examined numerically.
 - The RMS displacement is examined only, in which the non-trivial power law and log-periodic oscillations are observed.
 - The exponents are explained by the renormalization group argument applied both in the position and the reciprocal space.
2. Ref. [2]: I. Guarneri, "Spectral Properties of Quantum Diffusion on Discrete Lattices", Europhys. Lett. **10** (2), 95 (1989).
 - An analytical work, giving estimates for the RMS displacement (and in the bypass the mean occupation probability) under the diffusion in the fractal spectrum.
 - Here the expression for the correlation integral of the measure appears (first?) in relation to the wave packet expansion (i.e. not in Ref. [3]).
3. Ref. [3]: R. Ketzmerick, G. Petschel, and T. Geisel, "Slow Decay of Temporal Correlations in Quantum Systems with Cantor Spectra", Phys. Rev. Lett. **69**, 695 (1992).
 - The diagonal 1D tight-binding Harper and Fibonacci models are is examined numerically.
 - The system length is not indicated for numerics.

- The "auto-correlation function" $C(t)$, i.e. the mean probability $|\langle \psi(0) | \psi(t) \rangle|^2$ to find the initial state, is examined.
 - Some log-periodic features can be discerned in the plots, but are not discussed, since the power law is in the focus.
 - The explicit formulas are given relating $C(t)$ to the initial state measure auto-correlation integral, characterized by the correlation dimension D_2 .
4. Ref. [4]: I. Guarneri and G. Mantica, "Multifractal Energy Spectra and Their Dynamical Implications", Phys. Rev. Lett. **73**, 3379 (1994).
- Method is presented for the construction of a tri-diagonal matrix Hamiltonian with a prescribed scaling properties of the energy spectrum. So, this is something like the tight-binding model, but not clear what exactly (since the examples are not written down explicitly).
 - The constructed considered example (not written down explicitly) seem to posses uniform scaling properties over the spectrum, - due to the construction (but probably still multi-fractal (!) - since the WP expansion multi-fractality is still observed in the numerics) . For this example, moments $|x(t)|^q$ are calculated numerically for the initial state concentrated on a single "site", with the multi-scaling in the focus. Both multi-fractality. (in q) and the characteristic log-periodic oscillations are observed and noticed.
5. Ref. [5]: F. Piéchon, "Anomalous Diffusion Properties of Wave Packets on Quasiperiodic Chains", Phys. Rev. Lett. **76**, 4372 (1996).
- Theoretical (using the real space RG) and numerical paper on the multi-fractality of the WP expansion in 1D quasi-periodic Fibonacci and Harper tight-binding chain.
6. Ref. [6]: S. Thiem, M. Schreiber, and U. Grimm, "Wave packet dynamics, ergodicity, and localization in quasi-periodic chains", Phys. Rev. B **80**, 214203 (2009).
- The off-diagonal 1D tight-binding models are examined, with a quasi-periodicity due to the gold (Fibonacci), silver and bronze sequences.
 - The system length is several thousands of sites (~ 3000 -5000).
 - The RMS displacement and the "autocorrelation" $C(t)$ are examined.
 - LP oscillations are observed.
 - The kind of the strong-disorder PT (locator expansion) is applied to explain the results.
 - The additional point to pay attention is that the SILVER sequence seems to be preferable over the GOLDEN (Fibonacci) one to observe the LP features (see Fig. 3 herein). Also, some argumentation for the choice of the initial occupied site is given in terms of the RG theory (I think it is in this paper).
 - They also pay special attention to the "local exponents", which they use to describe the "power law" of a single log-periodic step. These quantities are independent of the strength of the modulation (probably for this reason authors believe they are important). On my opinion, these are not exponents at all: because they are defined on a very narrow interval of $\log t$, and also because they can be simply explained/modeled by a simple model with trifurcating spectrum with a controlled scaling factor like the Cantor set (I did it in Matlab). The later exhibits step-like structure for $C(t)$, which also has "local exponents" independent of the scaling factor (while the "global" one does depends), while the steep part of the step is just the finalization of the first period of the phase-destruction beat/stage at the relevant energy scale (i.e., it is not a "local" power law at all). On the other hand, they also appeal to some reference (No. 23 therein), where that kind of the exponent is discussed as well.
7. Ref. [7]: R. Lifshitz and S. Even-Dar Mandel, "Observation of log-periodic oscillations in the quantum dynamics of electrons on the one-dimensional Fibonacci quasicrystal", Phil. Mag. **91**, 2792 (2011).
- The off-diagonal 1D tight-binding Fibonacci model is examined by calculating the survival probability (same as "return" prob), the RMS displacement and the inverse participation ratio.
 - Relatively short systems are considered from 89 to 233 sites.
 - The power laws and the log-periodic oscillations are observed and discussed.
 - No analysis of the numerical results is presented.

8. Ref. [8]: S. Thiem and M. Schreiber, "Renormalization group approach for the wave packet dynamics in golden-mean and silver-mean labyrinth tilings", Phys. Rev. B **85**, 224205 (2012).
- 1-, 2- and 3-dimensional systems are considered numerically and an extended RG analysis is given to explain the exponents.
 - The off-diagonal tight-binding model are examined with a metallic-mean quasi-periodic ordering.
 - The RMS displacement is examined only (i.e. $C(t)$ is not).
 - The log-periodic oscillations are observed.
9. Y. Last, "Quantum Dynamics and Decompositions of Singular Continuous Spectra", J. of Functional Analysis **142**, 406 (1996).

This is a long mathematical paper dealing with the lower bounds on the wave packet expansion (a generalization of the Guarnerri bounds) in relation to the spectral properties, also with decomposition of the measures into the a.c., s.c. and point (etc.) parts.

B. System length (# of observed LPO periods vs Fibonacci generation)

1. Ref. [1]:
 - The off-diagonal 1D tight-binding Fibonacci model (2000 sites) is examined numerically.
2. Ref. [3]:
 - The system length is not indicated for numerics.
3. Ref. [6]:
 - The off-diagonal 1D tight-binding models are examined, with a quasi-periodicity due to the gold (Fibonacci), silver and bronze sequences.
 - The system length is several thousands of sites (~ 3000 -5000).
4. Ref. [7]:
 - The off-diagonal 1D tight-binding Fibonacci model with from 89 to 233 sites is examined by calculating the survival probability (same as "return" prob), the RMS displacement and the inverse participation ratio.
5. Ref. [8]:
 - 1-, 2- and 3-dimensional systems are considered numerically.
 - For 1D case the off-diagonal tight-binding model are examined with a metallic-mean quasi-periodic ordering with ??? (to check) sites.

C. Numerical experiment time scale vs energy scales of the spectrum

To accomplish...

D. Choice of the initial site position

To accomplish...

IV. THEORETICAL BACKGROUND

A. Usually considered quantities

The time evolution of the initial state (the wave packet) $\psi_0 \equiv \psi(t=0)$, $\|\psi_0\| = 1$, is considered. At later time t , it is given by

$$\psi(t) = \hat{G}(t) \psi_0, \quad (1)$$

where $\hat{G}(t) = e^{-i\hat{H}t}$, or by the implicit spectral decomposition

$$\psi(t) = \left[\begin{array}{l} \sum_n c_n \phi_n e^{-iE_n t}, \quad c_n \equiv \langle \phi_n | \psi_0 \rangle, \\ \int g(E) \phi(E) e^{-iEt} d\mu(E), \quad g(E) \equiv \langle \phi(E) | \psi_0 \rangle \end{array} \right], \quad (2)$$

where the first and the second lines correspond respectively to the discrete and the continuous formulations, and $\mu(E)$ is the spectral measure of the Hamiltonian.

To characterize the wave packet dynamics and to observe the fingerprints of the fractal spectrum (the power laws and the log-periodic features) in it, the following quantities are usually considered (see the literature review above):

1. The auto-correlation function, or the mean probability to find the system in the initial state (the mean "return/survival probability") (e.g. in [3])

$$C(t) \equiv \frac{1}{t} \int_0^t |\langle \psi_0 | \psi(t') \rangle|^2 dt'. \quad (3)$$

2. The RMS displacement

$$\Delta x(t) \equiv \sqrt{\langle (\hat{x}(t) - x_0)^2 \rangle} = \left[\int (\hat{x}(t) - x_0)^2 |\psi(t, x)|^2 dx \right]^{1/2}, \quad (4)$$

where for some reason people usually use the center x_0 of the initial wave packet instead of the mean position $\langle \hat{x}(t) \rangle$.

3. The time averaged participation ratio

$$\text{Pr}(t) = \frac{1}{t} \int_0^t dt' \left[\int |\psi(x, t')|^4 dx \right]^{-1}. \quad (5)$$

B. Auto-correlation function (mean return probability) $C(t)$

The time average is motivated as follows. The probability to find the system in the initial state (the "survival probability") at time t is

$$p(t) = |\langle \psi_0 | \psi(t) \rangle|^2 = \left[\begin{array}{l} \left| \sum_n |c_n|^2 e^{-iE_n t} \right|^2 \\ \left| \int |g(E)|^2 e^{-iEt} d\mu(E) \right|^2 = \left| \int e^{-iEt} d\mu_{\psi_0}(E) \right|^2, \quad d\mu_{\psi_0}(E) \equiv |g(E)|^2 d\mu(E) \end{array} \right] \quad (6)$$

is the absolute value of the Fourier transform of $|c_n|^2$ (discrete spectrum case) or the *spectral measure of the initial state* $\mu_{\psi_0}(E)$ (continuous case). Assuming some global scaling properties of the measure, one would get the corresponding scaling properties of $p(t)$ just by scaling of the integration variable (the following is "schematic" in a sense):

$$p(\lambda t) = \left| \int e^{-iE\lambda t} d\mu_{\psi_0}(E) \right|^2 = \left| \int e^{-iE't} d\mu_{\psi_0}\left(\frac{E'}{\lambda}\right) \right|^2 = \lambda^{2\beta} \left| \int e^{-iE't} d\mu_{\psi_0}(E') \right|^2.$$

Such an assumption is, probably, problematic for the measure $\mu_{\psi_0}(E)$ (which is normalized to unity), but can be (at least) imagined for $\mu(E)$ (which can be unlimited). Then, an approximate form of the scaling can probably be considered for $|g(E)|^2 d\mu(E)$ assuming some slow/special form of $|g(E)|^2$.

Even if the above-mentioned scaling can be considered analytically, the (real-valued) quantity $p(t)$ would usually exhibit fast (locally nearly periodic) oscillations, which would obscure the desired effects of the spectrum fractality. On the other hand, its time (Cezaro) average $C(t)$ becomes

$$C(t) \equiv \left[\frac{1}{t} \int_0^t dt' \sum_{n,m} |c_m|^2 |c_n|^2 e^{-i(E_n - E_m)t'} = \sum_{n,m} |c_m|^2 |c_n|^2 \frac{e^{-i(E_n - E_m)t} - 1}{-i(E_n - E_m)t} = \sum_{n,m} |c_m|^2 |c_n|^2 \text{sinc}((E_n - E_m)t) \right. \\ \left. \left| \int |g(E)|^2 e^{-iEt} d\mu(E) \right|^2 = \left| \int e^{-iEt} d\mu_{\psi_0}(E) \right|^2 = \int d\mu_{\psi_0}(E) \int d\mu_{\psi_0}(E') \text{sinc}((E - E')t) \right] \quad (7)$$

Here the use was made of $\frac{e^{-i\Delta Et} - 1}{-i\Delta Et} = e^{-i\Delta Et/2} \frac{2 \sin(\Delta Et/2)}{\Delta Et} = \frac{\sin(\Delta Et) - i \sin^2(\Delta Et/2)}{\Delta Et} = \text{sinc}(\Delta Et) - i \frac{\sin^2(\Delta Et/2)}{\Delta Et}$, while the anti-symmetric imaginary part must yield zero upon the summation/integration. Thus, the fast oscillations of $p(t)$ are suppressed by the time averaging in $C(t)$. Moreover, interpreting $\text{sinc}(\Delta Et)$ as a window function of the width t^{-1} , one recognizes (literally, - in the continuous version) a kind of the correlation integral of the spectral measure $\mu_{\psi_0}(E)$. The correlation integral of the measure μ is (e.g. Ref. [3, 9])

$$C(l, \mu) = \int_{E \times E} \theta(l - |x - y|) d\mu(x) d\mu(y), \quad (8)$$

where instead of $\text{sinc}(\Delta Et)$ there appears a rectangular window function (θ is a unit step function). The correlation dimension D_2 associated to $C(l, \mu)$ is defined then as

$$D_2 = \lim_{l \rightarrow 0} \frac{\ln C(l, \mu)}{\ln l}, \quad (9)$$

which for us means that for small l

$$C(l, \mu) \sim l^{D_2}. \quad (10)$$

The standard correlation integral $C(l, \mu)$ and $C(t)$ can be related using the Mellin transform with respect to l (or t), - like it was done in the similar situation for the wavelet transforms of the measures - see previous memos.

Thus, one expects (at least for large t) that

$$C(t) \sim t^{-D_2}, \quad (11)$$

but also the sub-leading log-periodic factor may be possible, - at least for some models of $\mu_{\psi_0}(E)$, i.e.

$$C(t) \sim t^{-D_2} F(\log t). \quad (12)$$

The question is whether this log-periodic feature is robust. To clarify the doubt, note that $C(t)$ can be interpreted also as a spectral average over $\mu_{\psi_0}(E)$ of the sinc-wavelet transform of the same measure (and by the initial state normalization $\int d\mu_{\psi_0}(E) = 1$). Thus, even if sinc-wavelet transform at each particular E' does exhibit the log-periodic modulation, it is not evident that this log-periodic feature would survive the spectral average if the measure is "multi-periodic" (in analogy to "multi-fractal"). On the other hand, the correlation dimension D_2 is probably due to some sub-set of the spectral points dominating the average, and, if that set has a uniform scaling period, then the log-periodicity should survive. The latter is supported by the following previous results (namely, local fractal exponent and the scaling period are related):

- Ashraff ('88): the scaling period is uniquely related to the exponent in off-diagonal (or mixed) tight-binding model (for same "p-cycle" of the RG).
- Wurtz ('88): the period and the exponent are uniquely related for same p -cycle in the optical super-lattice.

Relation to LDOS

In practice, as the initial state people usually take a single site population (in tight-binding model). Then the *spectral measure of the initial state* $\mu_{\psi_0}(E)$ becomes a local spectral measure (associated to the Local DOS $|\phi(n_0, E)|^2 \rho(E)$):

$$d\mu_{n_0}(E) \equiv d\mu_{\psi_0}(E) = |\phi(n_0, E)|^2 d\mu(E) \equiv d\mu_{n_0}(E), \quad (13)$$

where n_0 is the initially populated site (to be replaced with x_0 for the continuous coordinate). For that case $p(t)$ is the Green's function squared

$$p(t) = |\langle \psi_0 | \psi(t') \rangle|^2 = |G(x_0, x_0, t)|^2, \quad (14)$$

while the mean return probability

$$C(t) = \frac{1}{t} \int_0^t |G(x_0, x_0, t')|^2 dt'. \quad (15)$$

C. The RMS displacement and the participation ratio

In contrast to the mean return probability, it seems difficult to express the RMS displacement and the participation ratio in terms of the known standard quantities characterizing the fractal measures (like the correlation integral). To be continued ...

V. SOME PRELIMINARY NUMERICAL RESULTS

Initial wave packet (WP) of the width of about 2 letters, at $x_0 = 1420$ (letter length here is 20). The population is predominantly over the first sub-band:

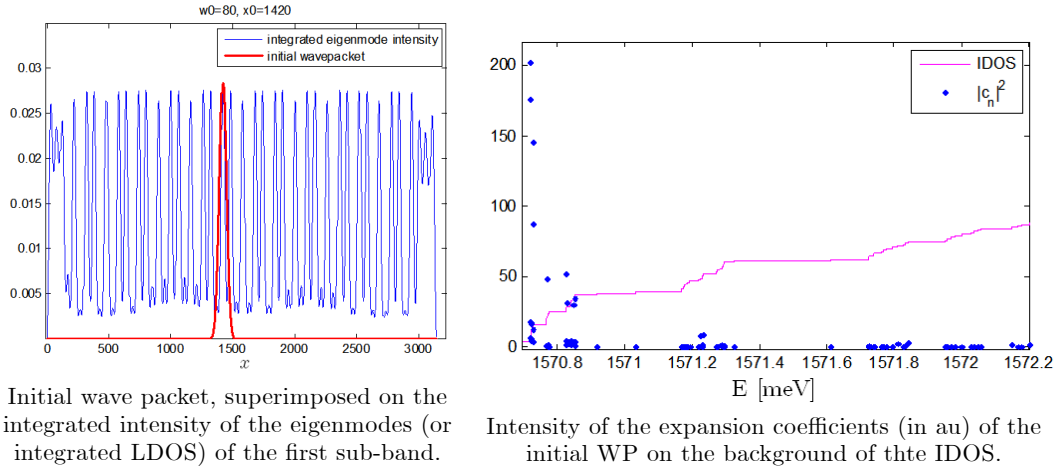


FIG. 2: Initial wave packet.

For this WP we obtain the following dynamics for $C(t) \equiv \frac{1}{t} \int_0^t |\psi(x_0, t')|^2 dt'$, and the width $\langle\langle x^2 \rangle\rangle$:

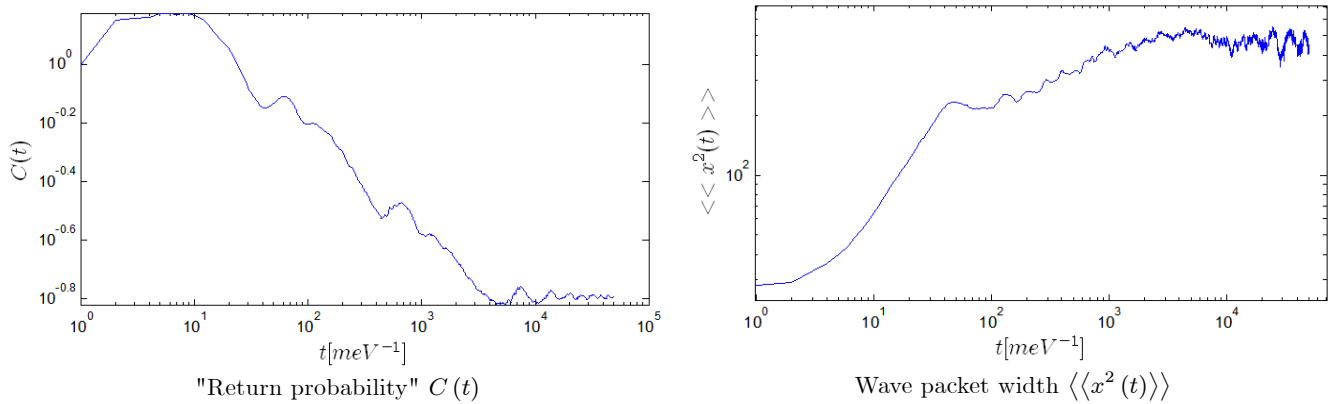


FIG. 3: Wave packet dynamics.

In $C(t)$ we clearly see three LP-periods with the scaling factors fitting those of the 1st sub-band spectrum. Those are not seen in $\langle\langle x^2 \rangle\rangle$, but, instead, there are some much more frequent oscillations from $t = 10^2 \text{ meV}^{-1}$ to $t = 10^4 \text{ meV}^{-1}$ (these oscillations are rather periodic, than nearly LP).

For the same initial packet, but somewhat different and more robust quantities. Namely

$$C(t) \rightarrow \frac{1}{t} \int_{x_0-\Delta}^{x_0+\Delta} dx \int_0^t |\psi(x, t')|^2 dt',$$

$$\langle\langle x^2 \rangle\rangle \rightarrow \langle(x - x_0)^2\rangle$$

where $\Delta = 10$ is half-letter length, are as follows

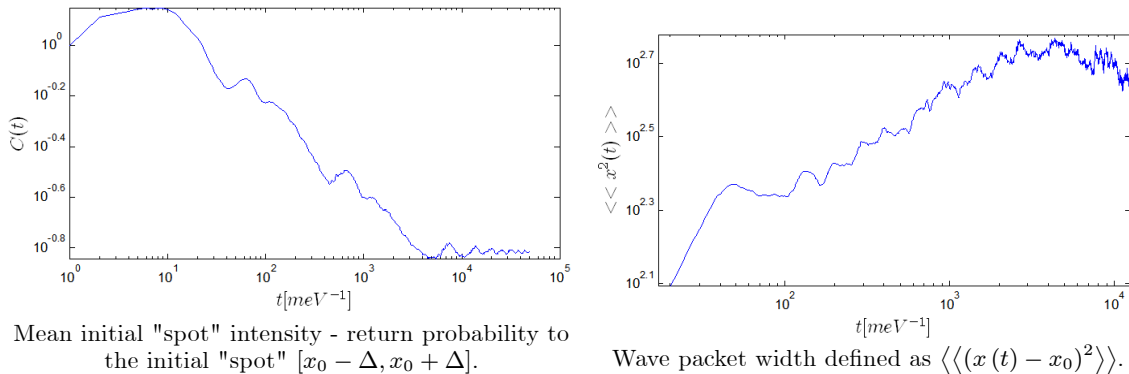


FIG. 4: Wave packet dynamics.

Thus, displacement $\langle(x - x_0)^2\rangle$ (usually used in literature) is somewhat better than $\langle\langle x^2 \rangle\rangle$. On the other hand, initial spot intensity is as good as the "return probability".

VI. SYSTEMATIC NUMERICAL SIMULATIONS

A. Method of numerical simulation

Initial state as a Gaussian wave packet with a given center x_0 and width w_0 ,

$$\psi(x, t = 0) \sim e^{-2(x-x_0)^2/w_0^2}. \quad (16)$$

Note that it does not necessarily describe correctly the initial state, which could be created in the polaritonic wire. This state is expanded into the eigenmodes ϕ_n of the system, and the state at the later time is obtained as

$$\psi(x, t) = \sum_n c_n \phi_n e^{iE_n t}. \quad (17)$$

The examined quantities are the time-averaged "return probability",

$$C(t) \equiv \frac{1}{t} \int_{x_0-\Delta}^{x_0+\Delta} dx \int_0^t |\psi(x, t')|^2 dt', \quad (18)$$

where Δ was set to half of a letter length, the RMS width, defined as

$$\Delta x \equiv \sqrt{\langle(x(t) - x_0)^2\rangle}, \quad (19)$$

which is somewhat different from the standard deviation, and the time-averaged participation ratio

$$\text{Pr}(t) = \frac{1}{t} \int_0^t dt' \left[\int |\psi(x, t')|^4 dx \right]^{-1}. \quad (20)$$

The choice of x_0 . To perform a systematic numerical calculation, several values of x_0 were chosen and for each one several initial widths w_0 were examined. The choices of x_0 are explained by Fig. 5 showing the map of the eigenfunction intensities. The guiding property is a desirable population of the modes, which depends both on x_0 and w_0 . Presumably, the ideal case is a uniform population of one of the main sub-bands, the first one - more realistically. (Then, the effect of the variation of w_0 around it can be considered.) Six values of x_0 were examined. Values $x_0 = 57.5, 68.5, 75.5, 78.5$ (in the units of the letter length) were chosen in a hope to "grasp" more states in the first sub-band using sufficiently large w_0 . Even if that worked to some extend, another two values $x_0 = 71.5, 73.5$ gave better results in terms of the target quantities.

Note: another consideration for the choice of x_0 is the renormalization group motivation. Namely, applying the RG iterations eventually leave a single site (letter) in tight-binding model. In some Ref. it is said that this site is in the middle of the original system (to be checked), which corresponds to $x_0 = 78.5$.

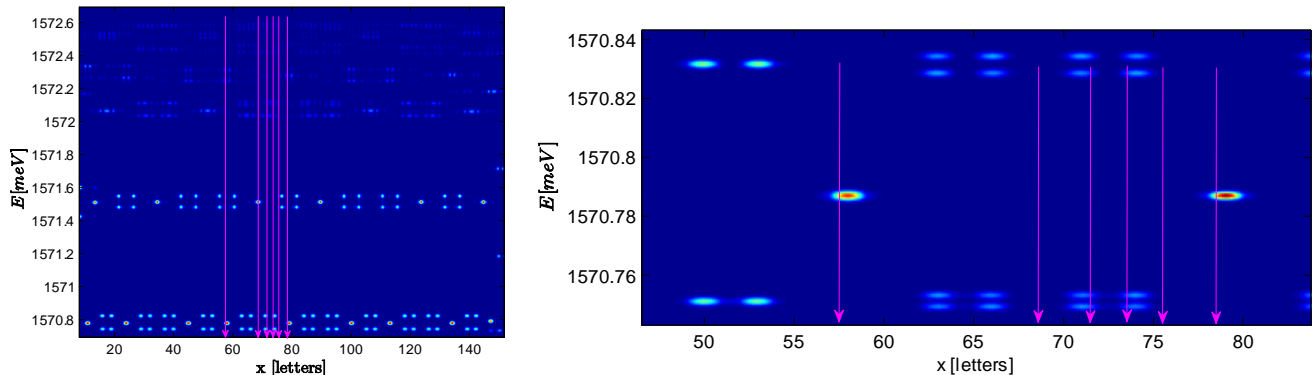


FIG. 5: Eigenfunction map and the choice of the initial wave packet centers. Left panel: the complete system length and the three main sub-bands are shown. Right panel gives zoom-in. Arrows show positions of the chosen values of x_0 .

B. Numerical results

The results are represented in Fig. 7, where each row corresponds to a given x_0 . First column shows the eigenmode population for different widths w_0 (in units of the letter length), by plotting the expansion coefficients $|c_n|^2$ (times 1000). Second column shows return probability $C(t)$, and the last one shows the RMS width and the mean participation ratio of the state.

Some Conclusions:

1. The desired effect of the discrete scaling symmetry of the spectrum is observed in the return probability $C(t)$ and the participation ratio $Pr(t)$, with three to four periods present (in accord with the expectation from the spectrum scaling, - see Fig. 1), while the RMS width does not show the log-periodic behavior. The RMS width, though does show some relevant features, like performing "constant" oscillations for some time, then increasing.
2. The specific dynamics strongly depends both on x_0 and w_0 . This was evident. The extreme case would be the choice of the initial state as one of the eigenstates, in which case there is no dynamics at all.
3. "Better" results are obtained for the values $x_0 = 71.5, 72.5$ (which are equivalent, - see Fig. 5). For those values, taking too narrow initial state, $w_0 = 1/4$, destroys the effect, since the population above the three sub-bands becomes significant. On the other hand, the "best" effect is obtained for $w_0 = 1$, which could be expected to be too small. Thus, population of all three main sub-bands is NOT a problem (as I thought). Probably, there is a separation of scales between the sub-bands (namely, smallest ones are present only in the first one). Otherwise, I would expect that different scaling factors of the different sub-bands would smear out the LP oscillations. Alternatively, I am wrong about "complete" multi-fractality of the spectrum, and there is some "dominant" scaling factor. Figure 6 shows that indeed the energy scales are different between the main sub-bands. Namely, Fig. 6 shows the level spacings. The gray markers represent the level spacing between the sequential eigenstates (i.e. all the eigenstates of the system). The important feature is the minimal level spacing in a given sub-band, since for the time $t > 2\pi/\Delta E_{\min}$ that sub-band does not have any non-trivial effect on the expansion dynamics. This is because the relative phases between its states, due to $\exp(-itE_n)$, are already "destroyed" at that time. Moreover, one actually need to examine level spacings between the states dominating the spectral expansion of

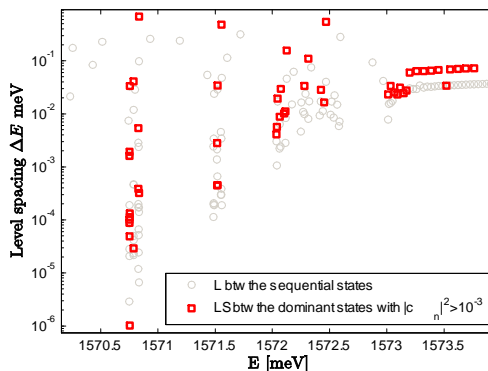


FIG. 6: Level Spacing

the initial wave packet. This is shown in Figure 6 for the initial states with $x_0 = 71.5$ and $w_0 = 1$ by plotting the level spacings only between the eigenstates with $|c_n|^2 > 10^{-3}$ (red squares). This demonstrates that:

- (a) The nontrivial dynamics can be observed till $t \sim 2\pi/10^{-4} \sim 10^5 \text{ meV}^{-1}$, - because the "typical" minimal LS in the first sub-band is of the order of 10^{-4} meV (the single LS 10^{-6} meV is not relevant).
 - (b) The second and the third sub-bands "quit the game" at earlier times by one order of magnitude each one (namely, the third sub-band has no effect after $t \sim 10^3 \text{ meV}^{-1}$ and, thus, does not interfere with the LP oscillations due to the scaling of the first and the second sub-bands; similarly for the second sub-band for the times later $t \sim 10^4 \text{ meV}^{-1}$).
 - (c) This separation of the LS scales explains why at long times we still observe one surviving period of the LP oscillations even for the very narrow initial state with $w_0 = 1/4$ (for $x_0 = 71.5$), - because the smallest LS are only in the first sub-band, which thus dominates the long-time decay of $C(t)$, even though its population is not dominant for such a narrow wave packet.
4. Still for $x_0 = 71.5, 72.5$, increasing w_0 above 1, freezes the WP for small times and, thus "hides" the first LP periods.
 5. The symmetry point, $x_0 = 78.5$ is not the preferential one (but check whether it is indeed such point).

The prominence of the LP features can be related to the "quality" of scaling of the LDOS at the chosen initial WP centers x_0 (Fig. 8(a)). Here the scaling is checked relative to the lower edge of the corresponding sub-bands, denoted by E_0 .

Figure 8(b,c) shows good scaling of LDOS also at position $x_0 = 60.5$, which was not expected from the visual inspection of the eigenmode map (there is series of other equivalent points). Fig. 9 shows expansion of the WP starting from this center. This time some features can also be found in the RMS displacement.

VII. SOME IDEAS

A. Resonant tunneling propagation and non-linear effects

The wave packet in the QP system propagates by resonant tunneling. This means that the wave function intensity moves from the initial spot to some distant ones without being large between them. This is in contrast to the usual diffusion in free space, where the intensity always decays monotonically away from the initial site. If the non-linearity is turned on, then its effect would be weak in the space between the resonant spots (where the intensity is always low), but can be significant on the resonant spots, where the intensity eventually increases. Does this give something interesting for the "lasing" of the polaritons in the QP wire?

B. Analogue of the spontaneous emission

As an analogue of the decay of a discrete system coupled to a fractal quasi-continuum, use square-well potential coupled to the Fibonacci chain. The eigenstate of the first can be tuned in resonance with one of the band of the

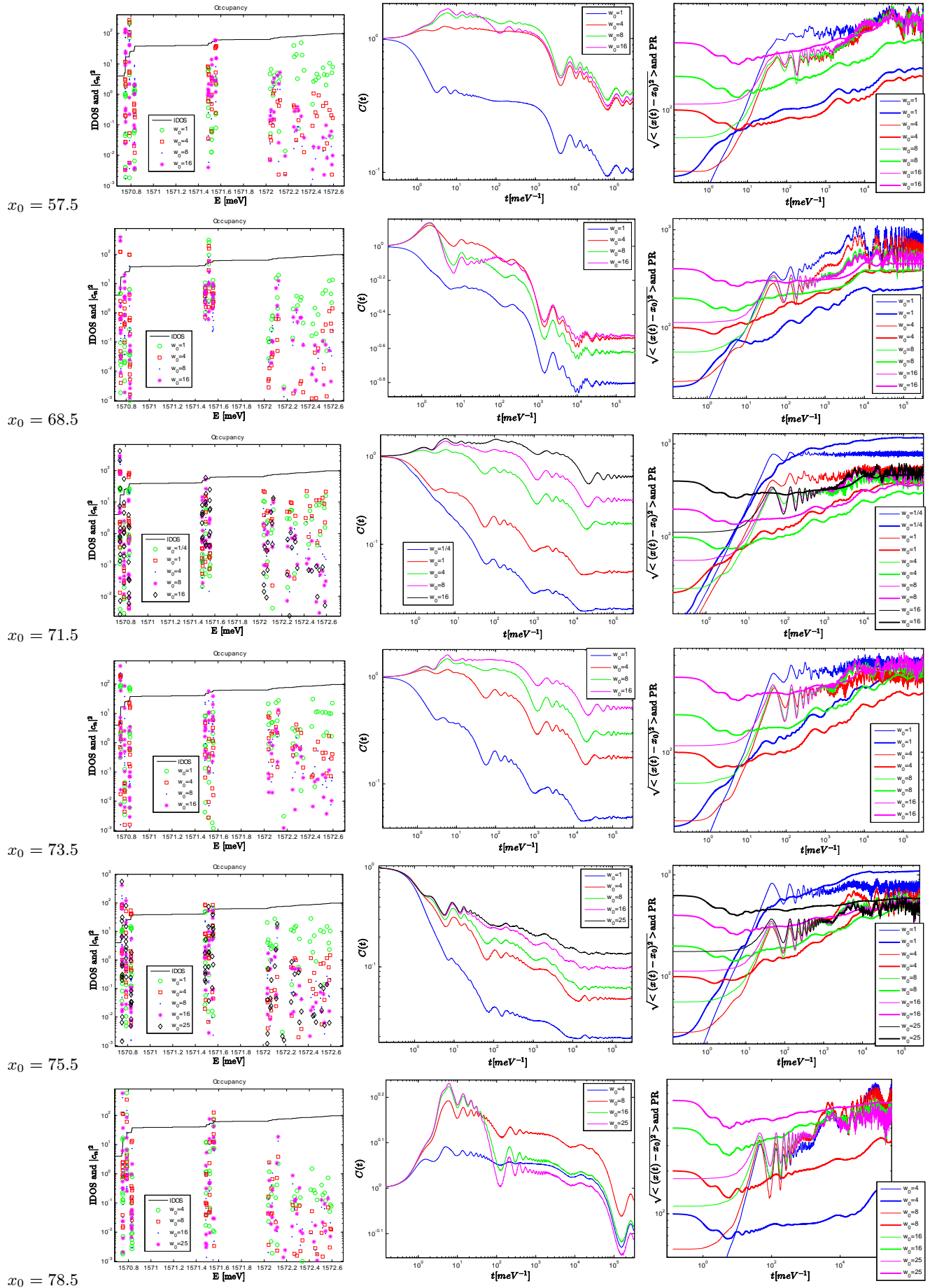


FIG. 7: Numerical results on the wave packet expansion.

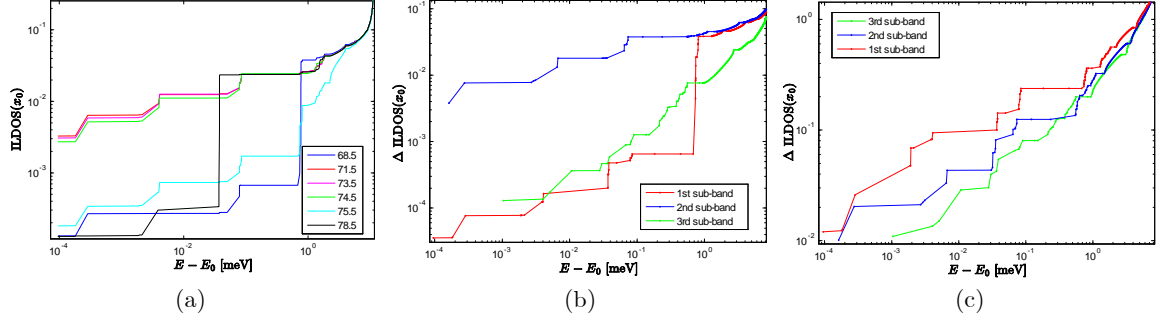


FIG. 8: Scaling of the integrated LDOS: (a) scaling of the first sub-band at different positions, (b) scaling for three sub-bands at $x_0 = 60.5$; (c) like (b) but LDOS is also integrated over the coordinate interval of a few letters.

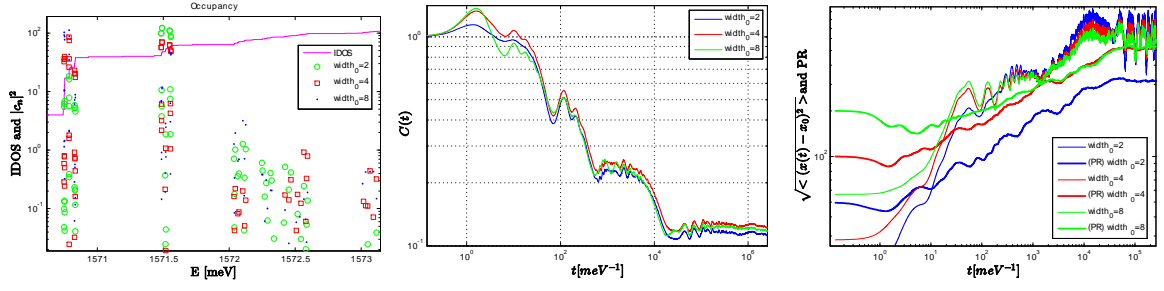


FIG. 9: Eigenfunction map and the choice of the initial wave packet centers. Left panel: the complete system length and the three main sub-bands are shown. Right panel gives zoom-in. Arrows show positions of the chosen values of x_0 .

Fibonacci chain. Then, the decay dynamics of the first can be expected to follow dynamics similar to that for the spontaneous emission.

Result: some preliminary numerics did not yield anything interesting.

-
- [1] S. Abe and H. Hiramoto, "Fractal dynamics of electron wave packets in one-dimensional quasiperiodic systems", Phys. Rev. A **36**, 5349 (1987).
 - [2] I. Guarneri, "Spectral Properties of Quantum Diffusion on Discrete Lattices", Europhys. Lett. **10** (2), 95 (1989).
 - [3] R. Ketzmerick, G. Petschel, and T. Geisel, "Slow Decay of Temporal Correlations in Quantum Systems with Cantor Spectra", Phys. Rev. Lett. **69**, 695 (1992).
 - [4] I. Guarneri and G. Mantica, "Multifractal Energy Spectra and Their Dynamical Implications", Phys. Rev. Lett. **73**, 3379 (1994).
 - [5] F. Piéchon, "Anomalous Diffusion Properties of Wave Packets on Quasiperiodic Chains", Phys. Rev. Lett. **76**, 4372 (1996).
 - [6] S. Thiem, M. Schreiber, and U. Grimm, "Wave packet dynamics, ergodicity, and localization in quasiperiodic chains", Phys. Rev. B **80**, 214203 (2009).
 - [7] R. Lifshitz and S. Even-Dar Mandel, "Observation of log-periodic oscillations in the quantum dynamics of electrons on the one-dimensional Fibonacci quasicrystal", Phil. Mag. **91**, 2792 (2011).
 - [8] S. Thiem and M. Schreiber, "Renormalization group approach for the wave packet dynamics in golden-mean and silver-mean labyrinth tilings", Phys. Rev. B **85**, 224205 (2012).
 - [9] D. Bessis, J. D. Fournier, G. Servizi, G. Turchetti, and S. Vaienti, Phys. Rev. A **36**, 920 (1987).